Article:
Xue, Y.-N., Li, Y.-X., Tang, Y.-M. et al. (6 more authors) (2025) Triclinic liquid crystal of counter-rotating squashed double helices in a side-chain polymer. Journal of the American Chemical Society. ISSN 0002-7863

https://doi.org/10.1021/jacs.5c02663

Triclinic liquid crystal of counter-rotating squashed double helices in a side-chain polymer

Yi-nan Xue[a], Ya-xin Li[b,*], Yu-min Tang[c], Shu-gui Yang[a], Ruo-yin Jia[b], Liliana Cseh[d], Feng Liu[a], Xiang-bing Zeng[c,*], and Goran Ungar[a,c,*]

[a] Shaanxi International Research Center for Soft Matter, State Key Laboratory for Mechanical Behaviour of Materials, Xi'an Jiaotong University, Xi'an 710049, China

[b] School of Chemistry and Chemical Engineering, Henan University of Technology, Zhengzhou 450001, China

[c] School of Chemical, Materials and Biological Engineering, University of Sheffield, Sheffield S1 3JD, U.K.

[d] Romanian Academy, Coriolan Dragulescu Institute of Chemistry, Timisoara 300223, Romania

ABSTRACT

A polysiloxane with tris-alkoxy-ended rod-like mesogenic side-groups forms an unusually low-symmetry antiferrochiral liquid crystal, spacegroup $P\bar{1}$, consisting of distorted left- and right-handed double-helices containing alternating splay and twist sections. The unit cell contains two double-helical columns. On faster cooling a closely related metastable orthorhombic structure is formed, symmetry *Fddd*, with 8 double helices per cell.

Keywords: Fddd phase, columnar, GISAXS, chiral, hemiphasmid, polycatenar

INTRODUCTION

Helical and especially double-helical structures in biological and synthetic systems have intrigued scientists and the general public ever since the discovery of the DNA double helix. Helix is a topological solution of a system's conflicting tendencies to order, hence form straight columns, and simultaneously avoid steric clashes. Thus most stereoregular polymers crystallize in a helical conformation, keeping the chains straight while avoiding side-group clashes, such as those of methyl groups in polypropylene.[1] Similar situations arise in "soft crystals" of complex molecules, including achiral ones, where homochirality of a helical column may propagate to long range due to the ordering influence from molecules on neighboring columns.[2,3]

High barrier between enantiomeric conformations may lead to quite long chiral correlation length even without a crystal lattice.[4,5,6,7,8,9,10] Helices can form from diverse achiral objects.[11] Concerning liquid crystals (LC), propagation of helical sense to true long-range order in achiral compounds has been known for some time in bent-core molecules.[12,13,14] Uniform twist in columnar phases of genuine LC character in achiral compounds has not been substantiated experimentally, since long-range order is unsupported in 1D.[15,16,17] Existence of uniform twist in a wider class of achiral LCs has been recognised when it was found that two of the three most common bicontinuous, network-based 3D phases of rod-like molecules are always chiral.[18,19] More recently it was found that a common mode of assembly of straight- or bent-rod polycatenar (multichain-bearing) molecules is in 3D orthorhombic arrays of alternating right- and left-handed helices with *Fddd* symmetry.[20,21,22] The long-pitch slow twist is a result of a balance between tendencies to maximise π-π attraction between aromatic rods and repulsion between the flexible end-chains.[20]

Here we report the first example of a LC phase of counter-twisting helices in a polymer. It turns out that here the stable structure is actually triclinic, the first example of such a low-symmetry LC in any system. The polycatenar moieties, tethered to both sides of an axial bundle of polymer backbones, describe a wide double helix. Its large size allowed us to "see" its actual structure through Fourier analysis of small-angle X-ray scattering (SAXS). We find that, contrary to previous LC and soft-crystal models and frequent cartoons, the helices are far from uniform. Instead they contain alternating nearly straight "splay" segments interrupted by sharply twisted "splay recovery" segments. This finding calls for re-evaluation of some established models of complex self-assembly.

RESULTS AND DISCUSSION

Polymer Si9-12 (Figure 1a) was synthesised by attaching 4-[3,4,5-*tri*(dodecan-1-yloxy)benzoate]-4'-[*p*-(nonan-1-yloxy)benzoate]biphenyl groups to a polymethylsiloxane backbone. The procedure was similar to that in ref. 23 and the details are given in Supporting Information (SI). Similar polymers with a propyloxy spacer and $C_5H_{11}O$ and $C_{12}H_{25}O$ end-chains were previously found to form smectic and columnar phases, respectively.[23] Chen et al. have recently studied side-chain LC polymers (SCLCP) with similar side-groups but with different backbones and found them forming mainly columnar phases.[24,25] SCLCPs are a diverse class of materials and combine application potentials of low-molar LCs with those of polymers.[26,27,28] E.g. SCLCPs can store optical, electronic or other alignment-based information by cooling below glass

transition and, if needed, erasing by laser heating or rewriting again above T_g.[27,29] SCLCPs have shown remarkable ability for thermal self-extension,[30] were used as high refractive index material,[31] as artificial muscles,[24] etc.

Si9-12 is found to form a hexagonal columnar (Col_h) phase at high temperatures and a new triclinic LC phase at lower temperatures (see below). The polymorphic transition is accompanied by a sharp DSC peak at 123°C on heating, 117°C on cooling, see Figures 1e and S1 in SI. Polarized optical micrographs (POM) in Figures 1b,c show typical developable domains ("spherulites") containing concentric circular columns. Figure 1c taken with the λ-plate, shows that the slow axis, i.e. the molecular axis, is radial, hence the mesogens are normal to column axis on average. Interestingly, the columns become less (negatively) birefringent with decreasing *T*, with a step reduction at the Col_h-Triclinic transition at 120°C (Figure 1d). No other change is seen in POM upon the transition (Figure S2).

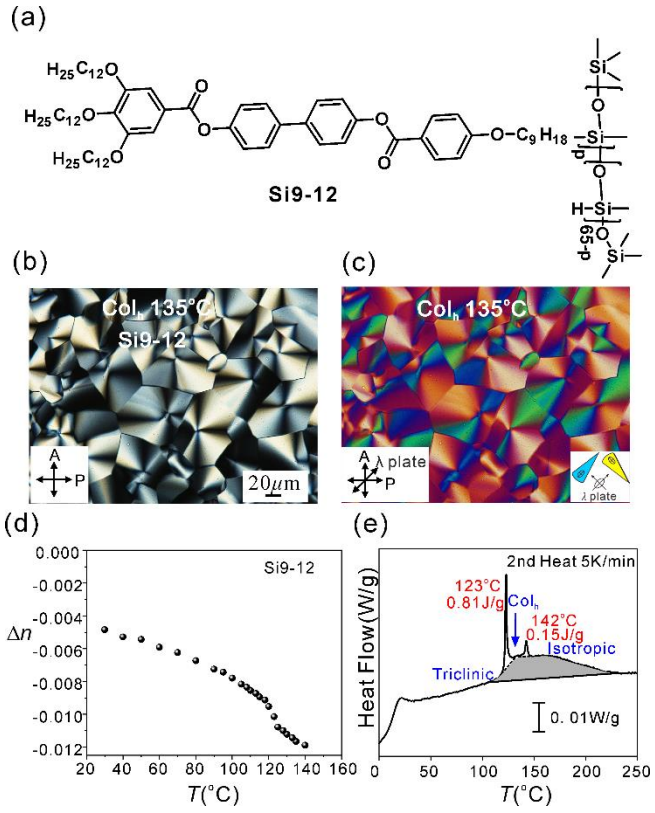

Figure 1. (a) Chemical structure of polymer Si9-12. According to NMR p=62. (b,c) POM of the Col_h phase without and with full-λ waveplate, respectively. (d) Birefringence n_e-n_o *vs.* temperature. (e) DSC thermogram, 2nd heating at 5 K/min.

Figure 2a shows a SAXS heating scan of a well-annealed sample. Throughout heating and cooling, the wide-angle scattering (WAXS) remains diffuse (Figure S6a,c). The high-*T* phase is clearly Col_h, since the q^2-values of Bragg peaks stand in

ratio 1:3:4 (Figure S3 and Table S1). See also the grazing-incidence (GISAXS) pattern in Figure S5. The complex powder pattern of the stable low-*T* phase is peak-resolved in Figure 2b. The indexing was based on the GISAXS pattern of thin film in Figure 2d. It was also facilitated by the fact that rapid cooling gave a simpler pattern (GISAXS in Figure 2c, powder in Figure S4). This metastable phase is orthorhombic, spacegroup *Fddd*,[20] with parameters *a*=28.19nm, *b*=16.28nm, *c*=8.99nm. GISAXS of the stable phase (Figure 2d) has many of the *Fddd* reflections split across the original layer-lines. The layer-lines are lost while row-lines remain. Thus the reciprocal *a**-axis is vertical, meaning that the real *bc*-plane lies horizontally on the substrate. Surprisingly, the symmetry is triclinic, lowest ever in a LC and, to our knowledge, in any soft non-crystalline system. With no systematic absences, the spacegroup is either *P*1 or $P\bar{1}$. Lattice parameters are *a*=9.44nm, *b*=16.89nm, *c*=9.24 nm, α=90°, β =117.7°, γ =120.0° (see Tables S2 and S3 for indexing the two phases). Note that the fact that α=90° is fortuitous. That the spacegroup of Triclinic phase is the centrosymmetric $P\bar{1}$ was ascertained by the absence of a second optical harmonic, expected at 470 nm (Figure S7).

Using diffraction intensities in Table S3 and Figure S4, 2D electron density (ED) map of the Col_h phase was constructed as shown in Figure 3a. Note the dip on top of the central peak, representing the low-ED column axis containing polymer backbone and nonyl spacer. This is surrounded by the high-ED aromatic mesogens (for values of ED for different parts of the molecule see Table S5). Top and side views of the model of a column are shown in Figure 3b. A column stratum 0.45nm thick (typical mesogen thickness) contains μ=12 monomer units (Table S4). The aromatic mesogens (high-ED) are shown spread in a cylinder around the column axis, which is threaded through by a bundle of ca. 12 polysiloxane backbones, flanked by the nonyl spacers. The outer dodecyl chains (low-ED) fill the remaining space.

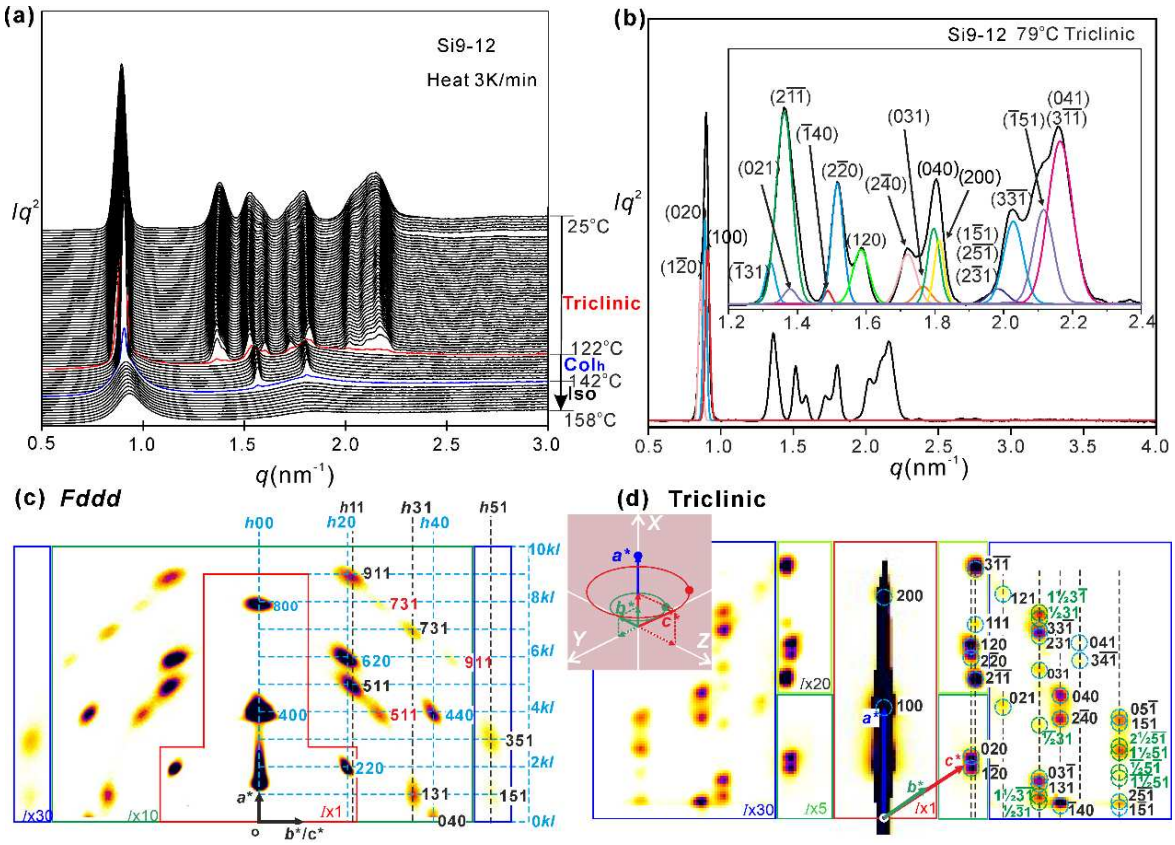

Figure 2. (a) Powder SAXS traces recorded during 3 K/min heating of Si9-12 previously cooled from Iso at 0.2 K/min. (b) Powder SAXS curve of Triclinic phase at 79°C. Inset: selected *q*-range with indexed peak-resolved components, with the ordinate scale expanded. (c) GISAXS at 25°C of *Fddd* phase in a rapidly cooled sample. Intensities in areas framed red, green and blue, respectively, are multiplied 1, 10 and 30 times. For the (100)-orientation: indices and row-lines *hk*0 blue, *hk*1 black; red indices are from alternatively orientated domains. (d) GISAXS of slow-cooled Triclinic film at 25°C. Intensities in areas framed red, green, yellow and blue are multiplied 1x, 5x, 20x and 30x. Spots with $h=n+1/2$ are circled and indexed green. Inset: reciprocal unit vectors *a*, b*, c** in space and their projections; real axes *X, Y, Z* are in white.

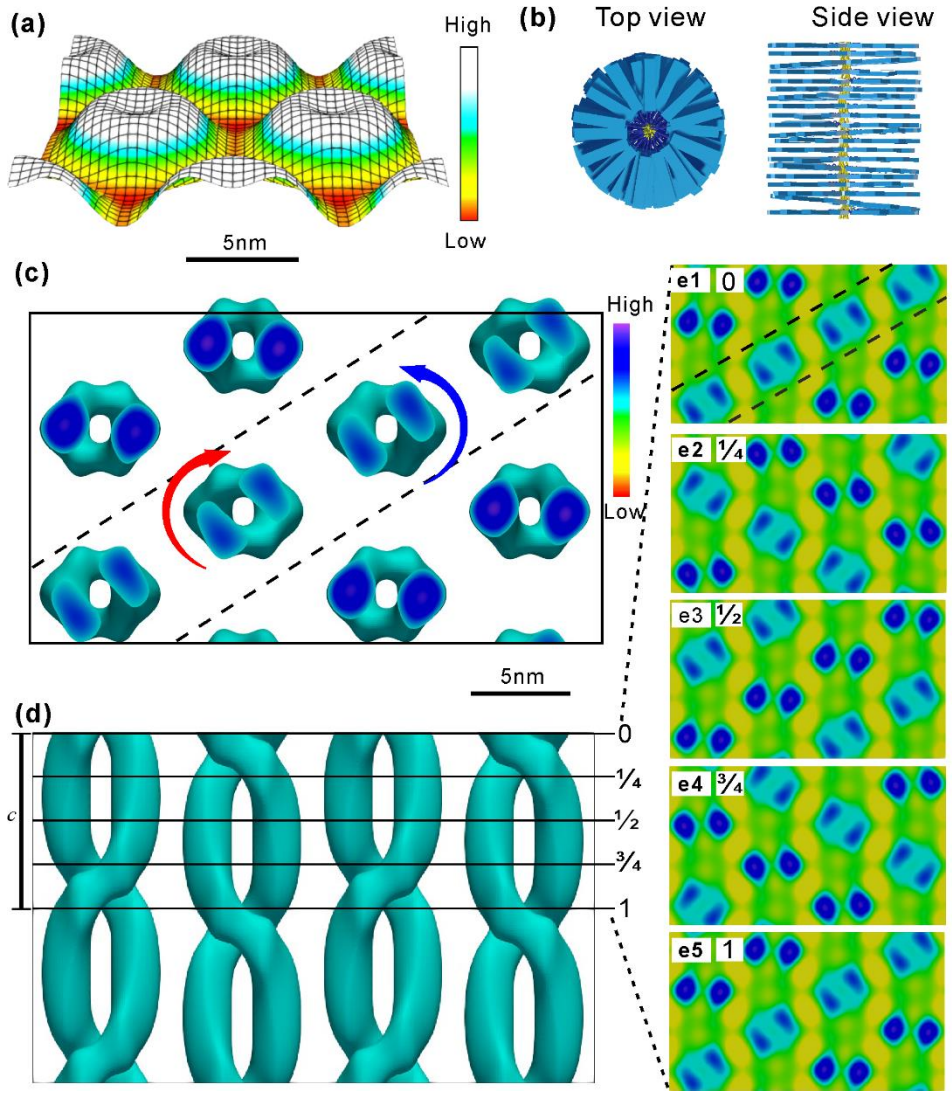

Figure 3. (a) Surface plot of 2D electron density map of the Col_h phase showing high-density rings (mesogens) with a low-density center (siloxane-spacer). (b) Top and side views of a Col_h column model. (c) Top view of ED map of an Fddd unit cell. (d) Side view of a row of 4 columns, two cells high, along the unit cell diagonal. In c,d isoelectron surface encloses the highest-ED volume, making up 16.5% of the total volume, or half the aromatic fraction. (e) *xy*-slices through the full ED map at increasing elevation labelled as fraction of *c*. c-e use the same color scale shown.

Figures 3c,d show top and side views of the 3D ED map of the *Fddd* phase, constructed using intensities and phases of the 12 strongest reflections shown in the powder diffractogram in Figure S4 and Table S3. See also Video 1. Phase selection was helped by recent structural studies of the *Fddd* phase in small molecules.[17,20] As in small straight- or bent-core polycatenars, there are 8 twisted columns in a unit cell, 4 right- and 4 left-handed. This is a prime example of an antiferrochiral phase.[17,20,32] Another antiferrochiral example is the gyroid cubic,

which consists of two antichiral networks, although it was shown recently that the gyroid can also have both of its networks of the same twist sense, thus being ferrochiral.[33]

Note that in Fddd successive columns along the diagonal (110) planes are antichiral whilst they are homochiral within (100) planes. Calculation, using a quadrupolar attraction-repulsion model, has shown that this packing mode is optimal.[20] It causes breaking of hexagonal symmetry, even though the column axes are on a 2D hexagonal lattice. The columns lie in the *bc*-plane which, as noted above, is mostly parallel to the substrate in GISAXS experiment.

However, comparison with the previous *Fddd* model in small molecules shows marked differences. Whereas there the columns are twisted single ribbons containing stacked rafts of 2-3 molecules located at the center of the column, in the polymer the aromatic mesogens (high-ED) form a double helix. In a stratum we find a raft of 6 mesogens in each helical strand, or total μ=12 mesogens per stratum, as in the high-*T* Col_h – see the model in Figures 4a,b, and Videos 2 and 3. The two helical strands are held to the central bundle of polysiloxane backbones by the nonyl spacers. The average twist between successive 0.45nm strata is $180\times0.45/c$=9.0°, comparable to that in small molecules. The pitch is 2*c*=18.5nm. The backbone braid is probably twisted such as to make the monomer repeat projected onto column axis match the 0.45nm stratum thickness.[34]

The wide double helices in the polymer allow us to “see” their more detailed structure. What Figures 3c-e show clearly is that the twist is anything but uniform. Instead the double helix is laterally squashed along *a*-axis, consisting of almost straight sections interrupted by sharp nearly 180° twists. This is seen clearly in Figure 3d and also in the sequence of *bc*-slices through the ED map in Figure 3e shown at intervals of *c*/4 along *c*-axis. The diagonal, delimited by dashed lines in e1, is the (110) row of columns in Figure 3d, where the *c*/4 slice positions are marked by horizontal lines. In Figures 3d,e each column is seen to perform a sharp twist at one of the *c*/4 levels.

As discussed previously,[17,20] the inter-raft twist is a balance between the need to avoid clash of end-chains while keeping the mesogens as parallel as possible to maximize their π-overlap. So what happens in the nearly straight sections of Si9-12 double-helix? The obvious answer is splay, as depicted in Figure 4b. The development of splay on cooling from Col_h to and through the double-helix phase is supported by birefringence becoming less negative (Figure 1d). No splay is needed in the idealized model of Col_h in Figure 3b since the mesogens are spread widely in the *ab* plane at random azimuthal angles.

Incidentally, splay is not an uncommon solution for accommodating bulging end-chains; it features in rectangular

columnar c2*mm* or *p*2*mm* "ribbon" phases and perforated layer "mesh" phases.[35] As a solution to the conflict between mesogen parallelism and end-chain avoidance in Si9-12, alternation of splay and twist zones seems better than a uniform twist, since in the splay zones π-overlap can still be well preserved. Only, of course, it cannot go on forever, and therefore periodic sharp twist zones are needed at *c*-intervals to reset the molecular tilt so splay can start anew. This structure also satisfies the polymer backbones' tendency for phase separation. An additional factor causing helix distortion must also be inter-columnar packing on a lattice. While here we can clearly see it, we believe distortion is a general feature of close-packed helices in soft matter.[34]

In reality, it is most likely that even in the Col_h phase local double-helical clusters had already formed with a continuous energy release on cooling as rafts of parallel mesogens continuously form. This aggregation probably starts already in isotropic melt, well above the Iso-Col_h transition. It would explain the broad heat capacity (C_p) maximum between >200°C and 123°C, shaded in Figure 1e. Such C_p maxima are common in the isotropic liquid above the transition to a complex mesophase, as pointed out recently.[36] There, using a statistical theory, we explained quantitatively such C_p anomalies being a result of continuous reversible formation of local aggregates. This also helps explain why the Col_h-Triclinic/*Fddd* transition enthalpy in Si9-12 is very small (0.3 - 0.8 J/g, depending on thermal history, Figures 1e and S1). This should be compared to around 10 J/g in small molecules, where no C_p anomaly is seen in the melt.[17,20] When the pre-ordering enthalpy of 8.3 J/g (shaded area in Figure 1e) is added to that of the two sharp transitions in Si9-12, we get a value close to 10 J/g, similar to that in small molecules. In other words, in the polymer most of the intermolecular bonding had already happened in the Iso melt.

So far the discussion was about the metastable *Fddd* phase. We now turn to the stable Triclinic. The Triclinic unit cell is shown from three different angles in Figure 4c. Although it is very different from the unit cell of *Fddd* and contains only two columns, the actual distortion of the orthorhombic packing is only slight. The red dashed lines in Figures 4c1-2 show the *Fddd* equivalent to the Triclinic cell. Molecular structure of the Triclinic phase is almost indistinguishable from that of the *Fddd*, but the distortion breaks the orthorhombic symmetry and allows slightly closer packing of the helices. To our knowledge this is the first reported triclinic LC. The lowest symmetry claimed that we are aware of is monoclinic.[37] We stress that the phase is a true liquid crystal, not a "soft crystal", as shown by the shape of the WAXS maximum, typical of liquids (Figure S6a,c). Normally, LCs with 2D or 3D order assume plane-groups or space-groups of highest symmetry, due to high motional freedom. However, the

constrained mesogen movement in a polymer can obviously bring down crystallographic symmetry of a LC to the lowest level.

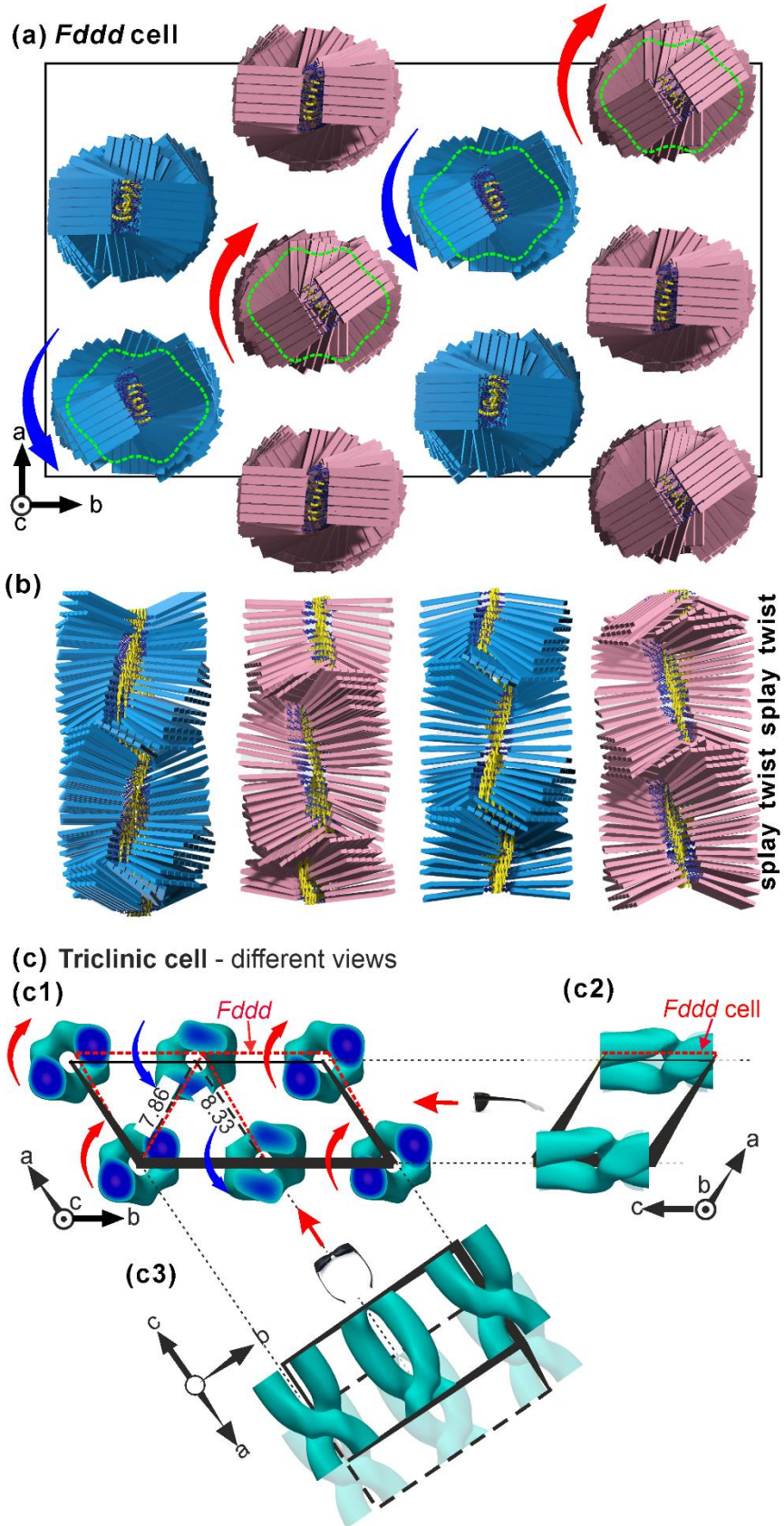

Fig 4. (a,b) Schematic model of the *Fddd* structure. (a) top view of a unit cell, (b) side view of columns along its diagonal. Prisms: aromatic mesogens, yellow: backbones, red (blue): Left-(right-)handed double-helices. In reality the 6-mesogen rafts are not meant to be either flat or distinct. (c) Different views of the 1-layer Triclinic unit cell. The spectacle icons define viewer's position and orientation. The distances in c1 are those of projections on plane of paper, in nm.

It is worth noting that braided structures with multiple helices have also been found in bent-core compounds, the most prominent being the B4 "helical nanofilament" (HNF).[38,39] However, HNF is based on twisted stacked layers, and is on a significantly larger lengthscale than the molecular scale in the system described here.

A final note on the few GISAXS reflections with half-integer *h*-index, circled green in Figure 2d. Their existence means that, strictly, the ultimate Triclinic unit cell, or "supercell", is twice the size of that described above, meaning that the *a*-parameter is actually 18.9nm. The supercell contains four columns in two layers. To give the green-circled reflections, the top layer must differ slightly from the bottom layer. However, the complete absence of (1/2 0 0) reflection (Figure 2d) means that the layer projections on their normal *a** are identical. This means that for alternating layers A and B there is a slight difference between A-B and B-A in-plane shifts. For GISAXS pattern with all-integer indices of the supercell see Figure S6b.

CONCLUSIONS

In summary, the cylinder-like columns of the high-temperature Col_h phase of this side-chain polymer transform on cooling to an array of antichiral double-helices. These deformed helices consist of alternating stretches of splay and twist, the two clash-avoiding modes normally found separately in different LC phases. While the metastable arrays are orthorhombic *Fddd*, the stable state is a uniquely low-symmetry Triclinic LC with a structure well approximated by an antiferrochiral unit cell with two counter-twisted columns. However, its true "supercell", also triclinic, contains four squashed double-helices. So far LC polymers have mostly mirrored the phases of low-molecular LCs, but this report, as well as our ongoing work, show that polymers offer new modes of self-assembly of their own.

ASSOCIATED CONTENT

Supporting Information

The Supporting Information is available free of charge at … It contains materials and methods, additional DSC, microscopy, XRD, SHG and X-ray diffraction data and analysis, and synthetic procedures with complete characterization data.

Additional data are deposited on Figshare at https://figshare.com/articles/dataset/Si9-12_indexing_triclinic_GISAXS/28374116, containing an excel file with calculation and the comparison of calculated and observed triclinic cell spacings, as well as the original NMR data.

Corresponding Authors:

g.ungar@xjtu.edu.cn, yaxinli@haut.edu.cn , x.zeng@sheffield.ac.uk

Note:

The authors declare no competing financial interest.

Acknowledgements:

For help with X-ray experiments we thank Dr. Olga Shebanova and Prof. Nick Terill of I22, and Prof. Steve Collins and Dr. Gareth Nisbet of I16, both at Diamond Light Source, as well as Drs Oier Bikondoa, Didier Wermeille, Paul Thompson and Laurence Bouchenoire of BM28 (XMaS) at European Synchrotron Radiation Facility. For such help we also thank the staff at beamline BL16B1 at Shanghai Synchrotron Radiation Facility. The work was supported by NSFC, China (92156013, 92356306, 22305068) and EPSRC, UK (EP-P002250). Part of the characterization was performed at Instrument Analysis Center of Xi'an Jiaotong University.

(1) de Rosa, C.; Auriemma, F. *Crystals and Crystallinity in Polymers*. John Wiley & Sons, Inc. 2014.

(2) Vera, F.; Serrano, J. L.; Sierra, T. Twists in mesomorphic columnar supramolecular assemblies. *Chem. Soc. Rev.* **2009**, *38*, 781-796.

(3) Partridge, B.E.; Wang, L.; Sahoo, D.; Olsen, J. T.; Leowanawat, P.; Roche, C.; Ferreira, H.; Reilly, K. J.; Zeng, X. B.; Ungar, G.; Heiney, P. A.; Graf, R.; Spiess, H. W.; Percec V. Sequence-Defined Dendrons Dictate Supramolecular Cogwheel Assembly of Dendronized Perylene Bisimides. *J. Am. Chem. Soc.* **2019,** *141***,** 15761−15766**.**

(4) Malthete, J.; Collet, A. Inversion of the Cyclotribenzylene Cone in a Columnar Mesophase: A Potential Way to Ferroelectric Materials. *J. Am. Chem. Soc*. **1987**, *109*, 7544–7545.

(5) Metzroth, T.; Hoffmann, A.; Martín-Rapún, R.; Smulders, M. M. J.; Pieterse, K.; Palmans, A. R. A.; Vekemans, J. A. J. M.; Meijer, E. W.;

Spiess, H, W.; Gauss, J. Unravelling the fine structure of stacked bipyridine diamine-derived C3-discotics as determined by X-ray diffraction, quantum-chemical calculations, Fast-MAS NMR and CD spectroscopy. *Chem. Sci.* **2011**, *2,* 69-76.

(6) Pisula, W.; Tomovic, Z.; Watson, M.D.; Muellen, K; Kussmann, J.; Ochsenfeld, C.; Metzroth, T.; Gauss, J. Helical Packing of Discotic Hexaphenyl Hexa-peri-hexabenzocoronenes: Theory and Experiment. J. Phys. Chem. B, **2007**, 111, 7481-7487.

(7) Aida, T.;Meijer, E.W. Supramolecular Polymers – we've Come Full Circle. *Isr. J. Chem.* **2020**, *60*, 33–47.

(8) Gearba, R.I.; Anokhin, D.V.; Ivanov, D.A. Elucidating the influence of side chains on the self-assembly of semi-flexible mesogens. *Chem. Commun.* **2025**, *61*, 282-285.

(9) Yashima, E.; Ousaka, N，; Taura, D。; Shimomura, K。; Ikai, T.; Maeda, K. Supramolecular Helical Systems: Helical Assemblies of Small Molecules, Foldamers, and Polymers with Chiral Amplification and their Functions. *Chem. Rev*. **2016**, *116*, 13752−13990.

(10) Lambov, M.; Hensiek, N.; Popler, A.C.; Lehmann, M. Columnar Liquid Crystals from Star-Shaped Conjugated Mesogens as Nano-Reservoirs for Small Acceptors. *ChemPlusChem* **2020**, *85*, 2219–2229.

(11) Chakrabarti, D.; Fejer, S.N.; Wales, D.J. Rational design of helical architectures. *Proc. Natl. Acad. Sci*. **2009**, *105*, 0906676106.

(12) Niori, T.; Sekine, T.; Watanabe, J.; Furukawa, T.; Takezoe, H. Distinct ferroelectric smectic liquid crystals consisting of banana shaped achiral molecules. *J. Mater. Chem*. **1996**, *6*, 1231-1233.

(13) Link, D.R.; Natale, G.; Shao, R.; Maclennan, J.E.; Clark, N.A.; Korblova, E.; Walba, D.M. Spontaneous Formation of Macroscopic Chiral Domains in a Fluid Smectic Phase of Achiral Molecules. *Science* **1997**, *278*, 1924-1927.

(14) Thisayukta, J.; Nakayama, Y.; Kawauchi, S ; Takezoe, H.; Watanabe, J. Distinct formation of a chiral smectic phase in achiral banana-shaped molecules with a central core based on a 2,7-dihydroxynaphthalene unit. *J. Am. Chem. Soc.* **2000**, *122*, 7441-7448.

(15) Savin A. V.; Manevitch L. I. Topological solitons in spiral polymeric macromolecules: A chain surrounded by immovable neighbors. *Phys. Rev. B* **2001**, *63*, 224303.

(16) Zagrovic, B. Helical signature motif in the fibre diffraction patterns of random-walk chains. *Mol. Phys.* **2007**, *105*, 1299-1306.

(17) Wang, Y.; Li, Y. X.; Cseh, L.; Chen, Y. X.; Yang, S. G.; Zeng, X. B.; Zhang, R. B.; Liu, F.; Hu, W. B.; Ungar, G. Enantiomers Self-Sort into Separate Counter-Twisted Ribbons of the *Fddd* Liquid Crystal - Antiferrochirality and Parachirality. *J. Am. Chem. Soc*. **2023**, *145*, 17443–17460.

(18) Dressel, C.; Liu, F.; Prehm, M.; Zeng, X. B.; Ungar, G.; Tschierske C. Dynamic mirror-symmetry breaking in bicontinuous cubic phases, *Angew. Chem. Int. Ed.* **2014**, *53*, 13115 –13120.

(19) H. J. Lu, X. B. Zeng, G. Ungar, C. Dressel, C. Tschierske "Solution of the Puzzle of Smectic-Q: The Phase Structure and the Origin of Spontaneous Chirality", *Angew. Chem. Int. Ed.* **2018**, *57*, 2835-2840.

(20) Li, Y. X.; Gao, H. F.; Zhang, R. B.; Gabana, K.; Chang, Q.; Gehring, G. A.; Cheng, X. H.; Zeng, X. B.; Ungar, G. A case of antiferrochirality in a liquid crystal phase of counter-rotating staircases**.** *Nature Commun.* **2022,** *13***,** 384.

(21) Rybak, P.; Krowczynski, A.; Szydlowska, J.; Pociecha, D.; Gorecka, E. Chiral Columns Forming a Lattice With A Giant Unit Cell. *Soft Matter* **2022**, *18,* 2006-2011.

(22) Li, Y. X.; Jia, R. Y.; Ungar, G.; Ma, T.; Zhao, K.; Zeng, X. B.; Cheng, X.H. Thermotropic "Plumber's nightmare" - A tight liquid organic double framework. *Angew. Chem. Int. Ed.* **2024**, *63*, e202413215.

(23) Percec, V.; Heck, J.; Ungar, G. Liquid crystalline polymers containing mesogenic units based on half-disc and rod-like moieties. 5. Side chain liquid crystalline polymethylsiloxanes containing hemiphasmidic mesogens based on 4-[3,4,5-tri(alkan-1-yloxy)benzoate]-4'-[p-(propan-1-yloxy)benzoate]biphenyl groups. *Macromolecules* **1991**, *24*, 4957-4962.

(24) Yang, Z.; Li, J.; Chen, X.; Fan, Y.; Huang, J.; Yu, H.; Yang, S.; Chen, E.-Q.. Precisely Controllable Artificial Muscle with Continuous Morphing based on "Breathing" of Supramolecular Columns. *Adv. Mater.* **2023**, *35*, e2211648.

(25) Zhao, R.; Zhao, T.; Jiang, X.; Liu, X.; Shi, D.; Liu, C.; Yang, S.; Chen, E. Q.. Thermoplastic High Strain Multishape Memory Polymer: Side-Chain Polynorbornene with Columnar Liquid Crystalline Phase. *Adv. Mater*. **2017**. *29*, 1605908.

(26) Finkelmann, H.; Rehage, G. Liquid crystal side chain polymers. In: Platé, N.A. (ed.) Liquid Crystal Polymers II/III. *Adv.Polymer Sci*. vol 60/61, Springer, Berlin, Heidelberg 1984.

(27) Shibaev, V. P.; Plate, N. A. Synthesis And Structure Of Liquid-Crystalline Side-Chain Polymers. *Pure Appl. Chem.* **1985**, *57*, 1589-1602.

(28) Kato, T.; Uchida, J.; Ichikawa, T.; Soberats, B. Functional liquid-crystalline polymers and supramolecular liquid crystals. *Polym. J.* **2017**, *50*, 149-166.

(29) Guardià, J.; Reina, J. A.; Giamberini, M.; Montané, X. An Up-to-Date Overview of Liquid Crystals and Liquid Crystal Polymers for Different Applications: A Review. *Polymers* **2024**, *16*, 2293.

(30) Kwon, Y. K.; Chvalun, S. N.; Blackwell, J.; Percec, V.; Heck, J. A. Effect of Temperature on the Supramolecular Tubular Structure in Oriented Fibers of a Poly(methacry1ate) with Tapered Side Groups, *Macromolecules* **1996,** *28,* 1552-1558.

(31) Yan, H.; Chen, S.; Lu, M.; Zhu, X.; Li, Y.; Wu, D.; Tu, Y.; Zhu, X. Side-chain fullerene polyesters: a new class of high refractive index polymers. *Mater. Horiz.* **2014**, *1*, 247–250.

(32) Zeng, Z.; Först, M.; Fechner, M.; Buzzi, M.; Amuah, E. B.; Putzke, C.; Moll, P. J. W.; Prabhakaran, D.; Radaelli, P. G.; Cavalleri, A. Photo-induced chirality in a nonchiral crystal. *Science* **2025**, *387*, 431-436.

(33) Wang, Y.; Yang, S.-G.; Li, Y.-X.; Cao, Y.; Liu, F.; Zeng, X.-B.; Cseh, L.; Ungar**, G.** Supertwisted Chiral Gyroid Mesophase in Chiral Rod-like Compounds. *Angew. Chem. Int. Ed*. **2024**, *63*, e202403156.

(34) Grason, G.M. Chiral and achiral mechanisms of self-limiting assembly of twisted bundles *Soft Matter* **2020**, *16*, 1102-1116.

(35) Ryu, J.-H.; Oh, N.-K.; Zin, W.-C.; Lee, M.-S. Self-Assembly of Rod-Coil Molecules into Molecular Length-Dependent Organization. *J. Am. Chem. Soc.* **2004**, *126*, 3551-3558.

(36) Xue, Y.N.; Zeng, X.B.; Wu, B.W.; Li, Y.X.; Cseh, L.; Liu, J.; Yang, S.G.; Gehring, G.A.; Liu, F.; Ungar, G. On the mechanism of soft self-assembly from melt: The ubiquitous heat capacity hump and spontaneous melt chirality. *Angew. Chem. Int. Ed.* **2025**, e202505548.

(37) Li, M.; Xu, J. R.; Zeng, Y.; Ben, H. J.; Yao, F. L.; Yang, S.; Chen, E. Q.; Ren, X. K. Ionic self-assembled derivatives of perylene diimide: Synthesis, aggregated structure and molecular packing behavior. *Dyes and Pigments* **2017**, *139*, 79-86.

(38) Hough, L. E.; Jung, H. T.; Krüerke, D.; Heberling, M. S. ; Nakata, M.; Jones, C. D.; Chen, D.; Link, D. R. ; Zasadzinski, J.; Heppke, G.; Rabe, J.P.; Stocker, W.; Körblova, E.; Walba, D. M.; Glaser, M. A.; Clark, N. A. Helical Nanofilament Phases. *Science* **2009**, *325*, 456–460.

(39) Shadpour, S. et al. Heliconical-layered nanocylinders (HLNCs) – hierarchical self-assembly in a unique B4 phase liquid crystal morphology. *Mater. Horiz.,* **2019**, 6, 959-968.

ToC Graphic